Integrating Spaceborne GNSS-R Measurements in 3D Ionospheric Imaging: A Simulation Study

Brenna Royersmith, Brian Breitsch, Y. Jade Morton
University of Colorado Boulder

SeNSe Lab — Satellite Navigation & Sensing Laboratory, University of Colorado Boulder

COLORADO CENTER FOR ASTRODYNAMICS RESEARCH

Abstract

This project focuses on the incorporation of GNSS reflectometry (GNSS-R) measurements obtained by low Earth orbiting (LEO) CubeSats in 3D ionosphere imaging using simulated data. The spatial and temporal resolution of tomographic images of the ionosphere is often limited due to the sparsity of ground-based receivers over oceans and polar regions, as well as the low number/coverage of GNSS radio occultation (RO). The goal of the project is to create an imaging method that will improve 3D imaging at high latitudes in both hemispheres using GNSS-R signals. Ionospheric image reconstruction is achieved using a voxel-based inversion technique. This method has been used to reconstruct a simulated 3D image of the ionosphere electron density using ground- and space-based satellite ray paths, including GNSS radio occultation and reflectometry signals. Resulting images are analyzed to evaluate the number of voxel intersections for different satellite geometries and assess image quality by quantifying reconstruction error. We show that incorporating GNSS-R increases the number of signal paths and improves the resolution and accuracy of resulting tomographic images. We then observe the relative impact of GNSS-R vs other signals on image quality, as well as explore geometries resulting from changes in satellite number or LEO constellation size/orientation. Results so far are promising for the future addition of real GNSS-R data to the program.

Background

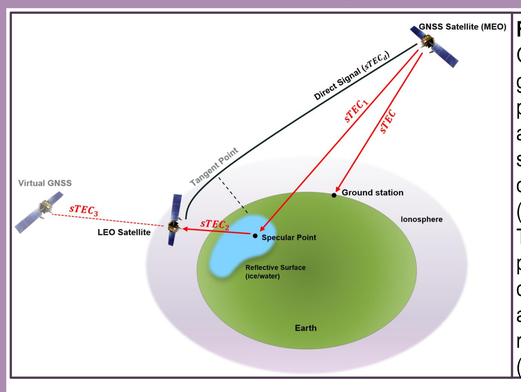

Figure 1. Example of GNSS-R[1] ray path geometry used in this project. Incorporated also are ground-based signals (sTEC), radio-occulted signals (GNSS-RO) (sTECd), TEC derived from precise orbit determination (sTEC3) and newly added reflected signals (STEC1 and 2).

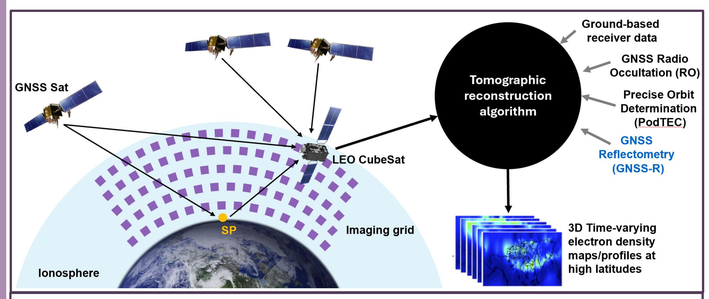

Figure 2. Example of the tomographic process[2]. A model ionosphere is used as a base (IRI). Data (simulated here) is collected by satellites as rays travel through the imaging area. These data are assimilated into an algorithm which sorts which measurements intersect the grid (voxels) and where, resulting in an updated model image which better reflects the real data and allows for more accurate images.

Inversion Method

Voxel-based inversion method:

- The ionosphere model base (IRI2016) is first broken into a grid of voxels.
- To keep voxels consistent in size and evenly distributed, stereographic coordinate systems are used in place of geographic (see **Figure 2**).
- A Voronoi forward method[3] is employed to find the voxel intersections of each ray path.
- Currently, this method searches the entire imaging area for intersections, but is being updated to only search a neighborhood around the ray to speed up calculation.

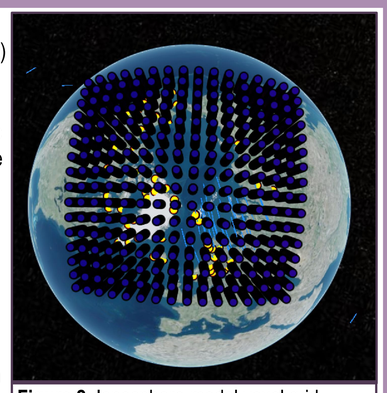

Figure 2. Ionosphere model voxel grid points over the north pole, shown in dark purple. Yellow markers are ground receivers.

- Inversion calculation of the ionospheric image is done using a simultaneous multiplicative algebraic reconstruction technique (SMART)[4]. Other studies utilize similar techniques such as ART, MART, or constrained (CMART)[5].

Figure 3. Visualization of how various ray path geometries travel through voxels (right) to aid understanding of the main inversion equation (left).

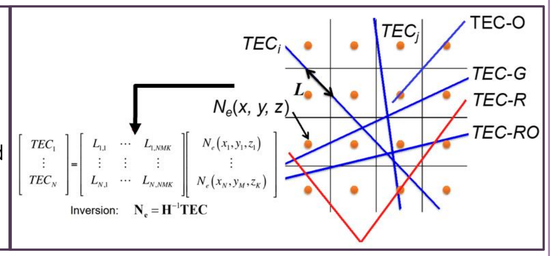

Tomographic Algorithm

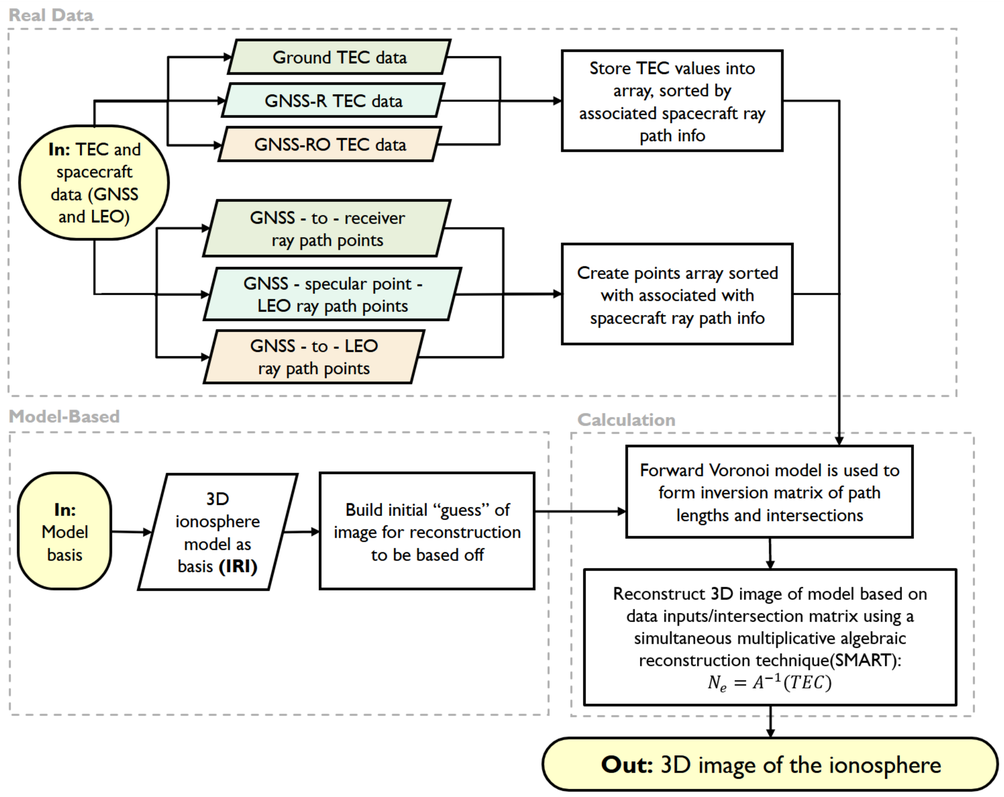

Figure 4. Block diagram explaining the process of our tomographic algorithm, from satellite data/information to resulting image.

Results

Satellite Simulation

- Satellite orbits are simulated based on real GNSS and Spire CubeSat orbital parameters (see **Table 1**)
- Reconstruction is run over a 30-minute period with a coarse grid of resolution 500km x 500km x 50km

Error in Reconstruction

- We define "error" as the difference between the base model and the reconstructed image
- Mean error refers to the average difference. RMSE is the root mean square of the difference.
- Columns of **Table 2** go as follows:
  - Number of GNSS satellites included
  - Number of LEO (Spire) satellites included
  - Number of rays which intersect the imaging area
  - RMSE of reconstruction, with reflected signals
  - Mean error of reconstruction with reflected signals
  - RMSE of reconstruction, without reflected signals
  - Mean error of reconstruction without reflected signals
  - Mean difference between with/without reflected signals

LEO Constellation	Number of CubeSats	Orbital Planes	Inclination (°)	Altitude (km)
Spire	24	6	97.3	500
GNSS Constellation	**Number of Satellites**	**Orbital Planes**	**Inclination (°)**	**Altitude (km)**
GPS	30	6	55	20,180
GLONASS	24	3	64.8	23,200
GALILEO	24	3	56	19,130
Ground Receivers	**Number of Receivers**	**Category**		**Latitude Cutoff (°)**
IGS	38	High latitude		55
CHAIN	16	High Latitude		55
Madrigal	29	High Latitude		60
SeNSe	5	High Latitude		55

Table 1. Orbital parameters for the GNSS and LEO constellations used in the simulation, as well as ground receiver information.

# GNSS	# LEO	Ray #	RMSE w/ GNSS-R ($1e9m^{-3}$)	ME w/ GNSS-R ($1e9m^{-3}$)	RMSE w/o GNSS-R ($1e9m^{-3}$)	ME w/o GNSS-R ($1e9m^{-3}$)	Mean Difference (ref - no ref)
5	1	1,004	11.87	4.46	11.87	4.46	0.00
15	5	3,498	13.39	6.57	13.59	6.67	0.09
30	10	10,239	12.34	5.86	12.90	6.11	0.25
45	15	18,868	9.95	4.66	11.26	5.25	0.59
60	20	30,901	8.36	3.72	10.24	4.64	0.92
78	24	44,224	8.04	3.42	10.04	4.45	1.04

Table 2. Collection of error/RMSE values comparing the addition of ray paths / reflection.

Slices of Resulting Images

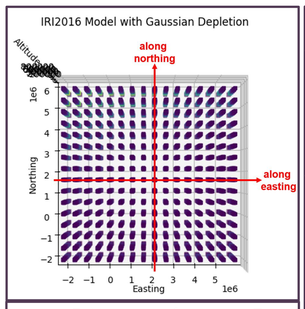

Figure 5. Visual aid for Figure 7 showing the imaging area grid in universal stereographic coordinates. This is the mesh which sits over the North Pole of the Earth with longitude 0 at the very bottom of the screen. Slices in Figure 7 are taken along the arrows shown, as well as across altitude.

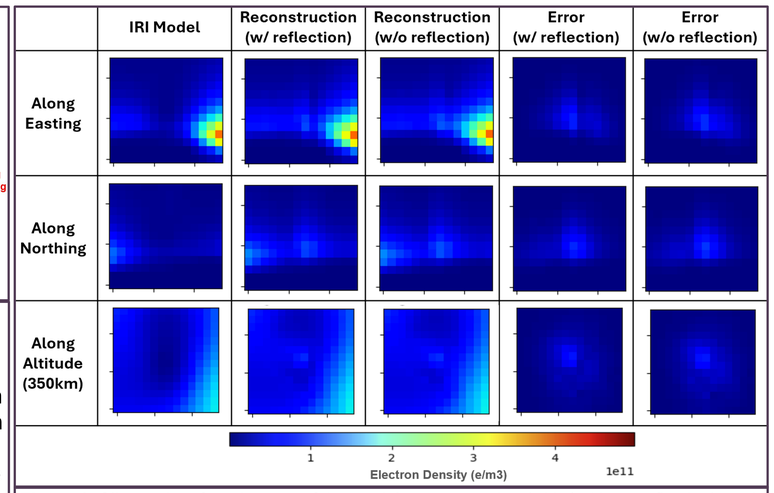

Figure 6. Slices taken from images of the model, reconstruction (with / without reflection), and error (with / without reflection) along each stereographic direction indicated in Figure 6.

Visualization

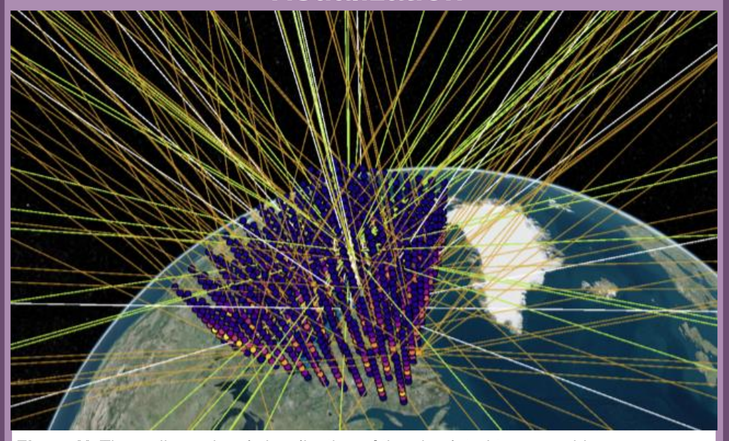

Figure X. Three-dimensional visualization of the simulated tomographic process using Cesium software. Figure produced by Brian Breitsch, software currently in use throughout project to assess program performance. White rays = ground-based, green rays = GNSS-RO, and orange rays = reflected.

Conclusions

1. The ionospheric tomography algorithm developed and used in this project is capable of producing three-dimensional images of the ionosphere given a base model and simulated satellites/electron density data. This leaves a starting point to grow from and improve upon.
2. Contrary to other tomographic methods, we utilize the addition of reflected signals with a forward Voronoi model for calculating voxel intersections, with a simultaneous multiplicative algebraic reconstruction technique for final image generation.
3. The addition of GNSS-R ray paths does improve image quality, but only marginally. We can also see that the more satellites we add, the more the image improves due to more voxel ray path intersections.
4. Simulation is very optimistic and idealistic, leading to questions about accuracy and feasibility. However, the results are still optimistic to the potential of this project.

Future Work:

- Detailed analysis of algorithm performance by studying how ray path number within a single voxel affects results and calculating statistics over cells with contain rays (remove those without any intersections)
- The addition of other, conceptual LEO CubeSat constellations to the reconstruction to further see how images improve with theoretically endless satellite geometries
- Update to IRI2020 to see if there are any changes to efficiency
- Study the possibility of adding covariance to reconstruction for regions with no data intersections
- Test on smaller (regional) and larger (global) scales to see how performances changes
- Real data processing

References

[1] C. Zuffada, C. Chew and S. V. Nghiem, "Global Navigation Satellite System Reflectometry (GNSS-R) algorithms for wetland observations," *2017 IEEE International Geoscience and Remote Sensing Symposium (IGARSS)*, Fort Worth, TX, USA, 2017, pp. 1126-1129, doi: 10.1109/IGARSS.2017.8127155.

[2] T. Hu, X. Xu and J. Luo, "A Global CIT Model Fusing Ground-Based GNSS and Space-Borne LEO Satellite Data for Monitoring the Geomagnetic Storm," in *IEEE Transactions on Geoscience and Remote Sensing*, vol. 62, pp. 1-11, 2024, Art no. 5801311, doi: 10.1109/TGRS.2024.3412953.

[3] Franz Aurenhammer. 1991. Voronoi diagrams—a survey of a fundamental geometric data structure. ACM Comput. Surv. 23, 3 (Sept. 1991), 345–405. https://doi.org/10.1145/116873.116880

[4] Gerzen, T. and Minkwitz, D.: Simultaneous multiplicative column-normalized method (SMART) for 3-D ionosphere tomography in comparison to other algebraic methods, Ann. Geophys., 34, 97–115, https://doi.org/10.5194/angeo-34-97-2016, 2016.

[5] Hui Li, Zhao Li, Baocheng Zhang, Chen Jiang, Xingliang Huo, 3D ionospheric tomography over southeast China using a new scheme of constrained least squares with parameter weight matrix, Journal of Atmospheric and Solar-Terrestrial Physics, Volume 203, 2020, 105255, ISSN 1364-6826, https://doi.org/10.1016/j.jastp.2020.105255.

Acknowledgements

This project is funded by ONR contract # N00014-23-1-2145.

Contact info:
Institution Email : Brenna.Royersmith@colorado.edu